

**A musculoskeletal model of the hand and wrist
model definition and evaluation**

Mirakhorlo, M.; Van Beek, N.; Wesseling, M.; Maas, H.; Veeger, H. E.J.; Jonkers, I.

DOI

[10.1080/10255842.2018.1490952](https://doi.org/10.1080/10255842.2018.1490952)

Publication date

2018

Document Version

Final published version

Published in

Computer Methods in Biomechanics and Biomedical Engineering

Citation (APA)

Mirakhorlo, M., Van Beek, N., Wesseling, M., Maas, H., Veeger, H. E. J., & Jonkers, I. (2018). A musculoskeletal model of the hand and wrist: model definition and evaluation. *Computer Methods in Biomechanics and Biomedical Engineering*, 21(9), 548-557.
<https://doi.org/10.1080/10255842.2018.1490952>

Important note

To cite this publication, please use the final published version (if applicable).
Please check the document version above.


Copyright

Other than for strictly personal use, it is not permitted to download, forward or distribute the text or part of it, without the consent of the author(s) and/or copyright holder(s), unless the work is under an open content license such as Creative Commons.

Takedown policy

Please contact us and provide details if you believe this document breaches copyrights.
We will remove access to the work immediately and investigate your claim.

A musculoskeletal model of the hand and wrist: model definition and evaluation

M. Mirakhorlo^a, N. Van Beek^a, M. Wesseling^b, H. Maas^a, H. E. J. Veeger^{a,c}  and I. Jonkers^b

^aDepartment of Human Movement Sciences, VU University, Amsterdam, the Netherlands; ^bDepartment of Human Movement Sciences, KU Leuven, Leuven, Belgium; ^cDepartment of Biomechanical Engineering, Delft University of Technology, Delft, the Netherlands

ABSTRACT

To improve our understanding on the neuromechanics of finger movements, a comprehensive musculoskeletal model is needed. The aim of this study was to build a musculoskeletal model of the hand and wrist, based on one consistent data set of the relevant anatomical parameters. We built and tested a model including the hand and wrist segments, as well as the muscles of the forearm and hand in OpenSim. In total, the model comprises 19 segments (with the carpal bones modeled as one segment) with 23 degrees of freedom and 43 muscles. All required anatomical input data, including bone masses and inertias, joint axis positions and orientations as well as muscle morphological parameters (i.e. PCSA, mass, optimal fiber length and tendon length) were obtained from one cadaver of which the data set was recently published. Model validity was investigated by first comparing computed muscle moment arms at the index finger metacarpophalangeal (MCP) joint and wrist joint to published reference values. Secondly, the muscle forces during pinching were computed using static optimization and compared to previously measured intraoperative reference values. Computed and measured moment arms of muscles at both index MCP and wrist showed high correlation coefficients ($r=0.88$ averaged across all muscles) and modest root mean square deviation (RMSD = 23% averaged across all muscles). Computed extrinsic flexor forces of the index finger during index pinch task were within one standard deviation of previously measured *in-vivo* tendon forces. These results provide an indication of model validity for use in estimating muscle forces during static tasks.

ARTICLE HISTORY

Received 26 July 2017
Accepted 16 June 2018

KEYWORDS



Finger; moment arm; pinch force

Introduction

A musculoskeletal model of the hand and wrist that includes intrinsic and extrinsic muscles, as well as the finger extensor mechanism can provide insight into hand function and motor control. Most of the available models are incomplete in a sense that they do not include the wrist joint or do not take into account the effect of the extrinsic finger muscles over that joint, or vice versa. It is well known that the relative position of the wrist has mechanical consequences on hand function; for instance on grip strength and finger motor control (O'Driscoll et al. 1992; Li 2002; Park et al. 2015). Hand function can therefore only limitedly be studied without accounting for the wrist mechanics.

Several musculoskeletal models consist of only one finger (Brook et al. 1995; Valero-Cuevas et al. 2000; Sancho-Bru et al. 2001; Wu et al. 2010; Allouch et al.

2015; Babikian et al. 2016) or focus solely on the thumb (Valero-Cuevas et al. 2003; Vigouroux et al. 2009; Wu et al. 2009). Recently more complete hand models were introduced, most of them still without including the wrist joint (Sancho-Bru et al. 2014; Vignais and Marin 2014; Lee et al. 2015; MacIntosh and Keir 2017). Recently, a finger and wrist model (Binder-Markey and Murray 2017) was presented, however, based on anatomical data derived from multiple sources and therefore scaled assuming a linear correlation with anthropometric data. This approach may not be justified for all parameters and may differ across muscle structures of the hand and fingers. For instance, considerably higher inter-subject variation for muscle mass and PCSAs of intrinsic muscles compared to extrinsic muscles has been reported (Jacobson et al. 1992). Considering the model sensitivity to these parameters (Ackland et al. 2012),

CONTACT Mojtaba Mirakhorlo  mirakhorlo@gmail.com  Department of Human Movement Sciences, VU University, Amsterdam, the Netherlands

© 2018 Informa UK Limited, trading as Taylor & Francis Group

This is an Open Access article distributed under the terms of the Creative Commons Attribution-NonCommercial-NoDerivatives License (<http://creativecommons.org/licenses/by-nc-nd/4.0/>), which permits non-commercial re-use, distribution, and reproduction in any medium, provided the original work is properly cited, and is not altered, transformed, or built upon in any way.

uniform scaling across muscles could be one of the reasons to impose unwanted inaccuracies to the model results. In a recent study, it was shown that using multiple instead of a single source for the anatomical parameters can lead to large (up to 180%) errors in muscle force prediction (De Monsabert et al. 2018). Therefore, there is a need for a musculoskeletal model of the hand and wrist that is based on a complete and consistent data set for the muscular parameters, therefore, alleviating the complexity of scaling. It should be noted that using a single cadaver limits the model in term of generalizability. Such a consistent data set was previously published by the authors (Mirakhorlo et al. 2016).

Another important feature of the hand and fingers is the extensor mechanism. This connective tissue structure connects the distal tendons of palmar interosseous, lumbrical and extensor digitorum muscles (Garcia-Elias et al. 1991). Due to this structure, intrinsic muscles exert flexion moments at the metacarpophalangeal (MCP) joints, but extension moments at the proximal interphalangeal (PIP) joints. This mechanisms mechanically couples the intrinsic muscles and distributes the forces exerted by the extrinsic extensor digitorum (Synek and Pahr 2016) and is typically modeled using a lateral and medial band (Valero-Cuevas et al. 1998).

Taking into account the wrist and using coherent input parameters are of great importance in modeling of the hand. The aim of the current study was to build a 3D model of the hand, which also includes a description of the wrist that is based on one consistent anatomical data set. Model performance was evaluated by comparing muscle moment arms at the index finger MCP joint and wrist joint, for which experimental data have been published (An et al. 1983; Kursa et al. 2005). In addition, tendon forces predicted by the model are compared to previously published experimentally obtained data sets (Kursa et al. 2005).

Methods

Model

The model was constructed using OpenSim 3.3 (Delp et al. 2007) comprising 22 segments including thumb (I), index (II), middle (III), ring (IV) and little (v) fingers with 26 degrees of freedom. The carpal bones were modeled as one single segment (see limitation part of the discussion for consequences of this simplification). All required anatomical input data including

bone masses and inertias, joint axis positions and orientations and muscle morphological parameters (including PCSA, mass, optimal fiber length and tendon length as well as muscle origins, insertions, via-points and wrapping surfaces) were obtained from a single cadaver data set (Mirakhorlo et al. 2016). As we have access to all the required parameters, there was no need to use any of the components of existing models available in the OpenSim, except for the bone geometries that were used for visualization purposes only.

Joints

The MCP joints have two degrees of freedom, allowing for flexion–extension and abduction–adduction. The PIP and distal interphalangeal (DIP) joints have one degree of freedom (flexion–extension). The thumb carpal-metacarpal (CMC) joint is modeled as a saddle joint connecting metacarpal bones to the carpals with two degrees of freedom (flexion–extension and abduction–adduction). The carpal segment, linked to the ulna as a saddle joint, allows the flexion–extension and radial/ulnar deviation relative to the wrist. This simplified modeling of wrist, in contrast to more realistic modeling (Fischli et al. 2009; Majors and Wayne 2011) that accounts for complex kinematics of the human wrist, may affect the outcomes of the model, as elaborated in the limitation section of discussion. A joint with one degree of freedom connects the ulna and radius enabling forearm pronation/supination.

Muscles

All 43 muscle-tendon units have been defined as line segments (Figure 1(a)) with cylindrical wrapping surfaces for MCP, PIP and DIP joints. Maximum isometric muscle forces have been calculated based on the PCSAs, considering a specific tension of 55 N/cm²,

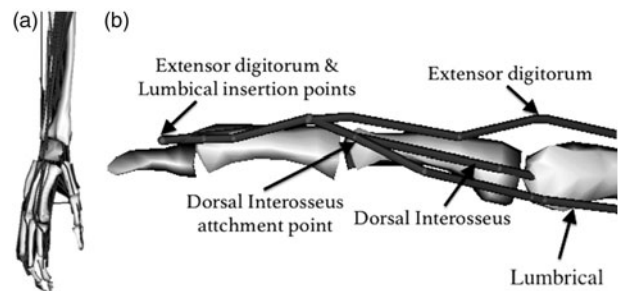


Figure 1. Tendon paths of all muscles (a) and the structure of the extensor mechanism of the index finger (b). Gray surfaces represent bone segments; these surfaces are shown for visualization purposes only.

which is obtained from an *in-vivo* human study (O'Brien et al. 2010). Since multiple attachment points are available in our data set for the extensor mechanism, these are modeled using separate paths, sharing via-points particularly in the distal region of the extensor mechanism analogous to its medial bands (Valero-Cuevas et al. 1998) (Figure 1(b)). Unlike the medial bands, the lateral bands require multiple insertions for a single muscle-tendon unit path model, which is not feasible in OpenSim. Therefore, the lateral bands of the extensor mechanism were not included in the model.

Modification and scaling

As the attachment points of lumbricals III and IV were missing from the anatomical data set due to technical problems explained in (Mirakhorlo et al. 2016), the paths of these muscles were estimated by scaling based on the attachment points of the first lumbrical and the lengths of the index, middle and ring phalanges. Furthermore, due to lack of sufficient via-points in the data set for flexor digitorum superficialis (FDS) II and III, flexor digitorum profundus (FDP) IV, extensor digitorum (ED) II, ED IV, ED V (See Table 1 for abbreviations), an additional via point, in the middle between two measured via points located at metacarpal and proximal phalange, was added for all muscles mentioned above.

To accommodate for a discrepancy in the total length of the modeled muscle elements compared to the measured ones (Mirakhorlo et al. 2016), mainly because of simplification of the muscle-tendon units to straight lines, a scaling step was applied to the actual measured fiber and tendon slack lengths in order to achieve active muscle force production for the whole range of finger and wrist motion. Therefore, both experimentally measured tendon slack lengths and a fiber length of each individual muscle were scaled based on a scaling factor derived from the total muscle-tendon length computed by OpenSim and the experimentally measured total muscle-tendon length. The scaling procedure was verified by evaluating the active force exerted by the extrinsic finger flexors (FDS and FDP) in the neutral

anatomical position (with all joint angles at 0°) and in the maximally flexed position: wrist flexion: 75° (Günel et al. 1996), MCP: 90°, PIP: 101° and DIP: 84° (Bain et al. 2014). Except for the modified and scaled parameters, all the other experimentally measured anatomical parameters were implemented in the model without any changes.

Comparison with experimental data

Moment arms during finger and wrist flexion/extension

We computed the moment arms of muscles crossing index finger for MCP, PIP and DIP flexion over a range of motion of 90°, 90° and 55°, respectively. These ranges were selected similar to the ranges of a previous experimental study (An et al. 1983) to which the computed moment arms were compared. Patterns and values were compared with experimentally derived moment arms of the index finger MCP joint for one representative cadaver (out of seven) during MCP flexion (An et al. 1983). An et al. (1983) provided the angle-dependent moment arms only for one cadaver and only during MCP flexion. The computed moment arms were compared to the mean moment arms of MCP, PIP and DIP joints averaged over the imposed range of joint movement. For all four fingers, the moment arms were computed at the MCP, PIP and DIP joints. Only some basic anthropometric measurements, length, and thickness of phalanx, are available for both An et al. (1983) and the cadaver dissected for the anatomical data as the model input (Mirakhorlo et al. 2016). There were some differences in the length of phalanx between the cadavers studied in An et al. (1983) and (Mirakhorlo et al. 2016) that is up to 2 mm in middle phalanx length, which may limit the comparison of the model's outcome and An et al. (1983) moment arms (see Discussion section).

In addition, wrist flexion–extension moment arms were computed for the muscles crossing the wrist (ECRL, ECRB, ECU, FCR, and FCU) and the extrinsic finger flexors (FDS II–IV and FDP II–IV). These were compared with previously published moment arms (Loren et al. 1996; Brand and Hollister 1999). As Loren et al. (1996) only presented lower and upper bands of the moment arms of the wrist muscles, the estimated average curve was used. To our knowledge, no experimentally measured moment arms of the extrinsic finger extensors (ED and EDI) at the wrist have been published.

Table 1. Muscle abbreviations.

EI	Extensor indicis	ECRL	Extensor carpi radialis longus
ED	Extensor digitorum	ECRB	Extensor carpi radialis brevis
FDS	Flexor digitorum superficialis	ECU	Extensor carpi ulnaris
FDP	Flexor digitorum profundus	FCR	Flexor carpi radialis
LU	Lumbricales	FCU	Flexor carpi ulnaris
PI	Palmar interosseus		
DI	Dorsal interosseus		

Calculation of pinch force

Muscle forces during pinching were computed and compared to intraoperatively measured FDS and FDP tendon forces during slow rate loaded pinching (Kursa et al. 2005) in which subjects were instructed to exert force in slow, medium and fast rate loading conditions equal to 1.5, 5 and 15 N/s. Kursa et al. (2005) reported the ratio of FDP and FDS forces to the applied fingertip force, hence, these ratios were also calculated from the model results. Finger joint angles of the model were set to the mean angles reported (MCP: 33°, PIP: 51° and DIP: 54°) with wrist angle at 15° at extension and pinch forces were applied ranging between 2 and 10 N at an angle of 60° to the fingertip (Kursa et al. 2005). As the point of force application on the fingertip was not reported, it was estimated based on the provided figure (Figure 1 in Kursa et al. 2005), using the dimension of the force sensor for calibration, being 22 mm distally from the DIP joint. Static optimization, as implemented in OpenSim, was used to estimate the individual muscle-tendon forces that counterbalanced the external moment using the only available cost function in OpenSim (i.e. $\sum_1^n \alpha^p$); where α = muscle activation and using $p=3$. All implemented muscles

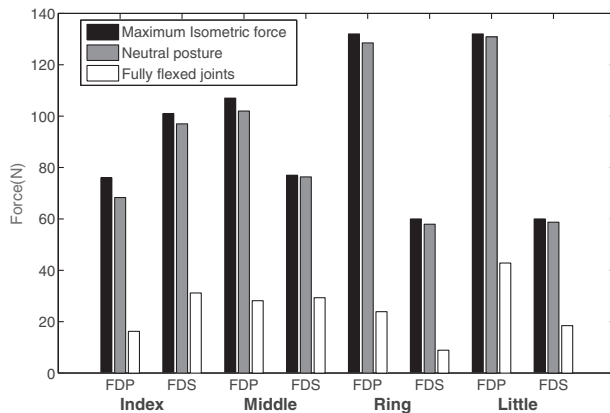


Figure 2. Theoretically maximum isometric muscle forces and calculated forces in the neutral hand position (joint angles at 0°) and fully flexed position (wrist: 75°, MCP: 90°, PIP: 101°, DIP: 84°)

were involved in optimization and all degrees of freedom of index finger and wrist were included in the inverse dynamics analysis.

Analysis

To compare model and experimental moment arms during MCP flexion of the index finger and wrist flexion/extension, correlation coefficients (r) and root mean square deviation (RMSD) were calculated. For the moment arms at the wrist, RMSD and r -values of FDS and FDP were averaged across fingers II–V. The ratio of computed muscle-tendon forces to the fingertip force during the pinch task was compared with the experimental measurements (Kursa et al. 2005). All calculations were performed in Matlab (2014, Mathworks).

Results

Muscle active force production

In a maximally flexed position, the muscle fibers of the extrinsic flexors (FDS and FDP) still produce active force, but considerably lower than in the neutral position (Figure 2). Furthermore, the active muscle forces in the neutral anatomical position were only slightly lower (0–5 N) than the theoretical maximum isometric forces (calculated based on PCSAs and the specific tension) (Figure 2).

Moment arm evaluation

For both the intrinsic and the extrinsic muscles ($r > 0.83$ and > 0.93 ; Table 2) high correlation coefficients between the computed and experimentally derived moment arms (An et al. 1983) were found. The magnitudes of moment arms were quite similar to the extrinsic muscles (Figure 3a); RMSD ranged from 8.7 to 15.4% (Table 2), and were substantially less similar for the intrinsic muscles; RMSD ranged between 19 and 61% (Table 2 and Figure 3b).

Muscle (Wrist) ECRBECRL

The mean flexion–extension moment arms of the muscles crossing the MCP, PIP and DIP joints of the

Table 2. Correlation coefficients between model and experimental flexion–extension moment arms of the index MCP joint during MCP flexion and of the wrist joint during wrist flexion–extension ($p < 0.001$) (see Table 1 for abbreviations).

Muscle (Index)	ED II	EI	FDS II	FDP II	LU I	DI I	PI II
Correlation (r)	0.87	0.83	0.98	0.97	0.94	0.93	0.97
RMSD (%)	12.8	8.7	9.8	15.4	27.52	61.1	19.54
Muscle (Wrist)	ECRB	ECRL	ECU	FCU	FCR	FDS	FDP
Correlation (r)	0.97	0.99	0.75	0.51	0.69	0.98 ^a	0.98 ^a
RMSD (%)	19.4	31.2	41.6	18.5	13.5	15.4 ^a	34.7 ^a

^aAveraged for all fingers (II–V).

index finger were similar to those measured experimentally (An et al. 1979) (Table 2). Only the computed moment arm of the lumbrical at MCP was considerably lower than experimental measurements (An et al. 1979).

The patterns of the moment arms for ECRB, ECRL, FDP and FDS at the wrist joint during wrist flexion–extension were similar to the experimentally obtained data from the literature (Figure 4; $r > 0.97$; Table 2). For the ECRB and FDS, the mean deviation from experimental moment arms (RMSD) was modest (19 and 15%, respectively). However, the error for ECRL and FDP RMSDs were higher (31.2 and 34.7%, respectively; Table 2). The level of similarity was low for ECU, FCR and FCU. Correlation coefficients (r value) were 0.75, 0.69 and 0.51 for ECU, FCR and FCU, respectively. The deviations for FCR and FCU were small (RMSD $< 15.4\%$), but large for ECU (41.6%; Table 2).

Computed muscle moment arms for all fingers and joints

For each muscle, the joint angle–moment arm curves were quite similar across fingers (Figure 5). The intrinsic muscles except for DI act as an extensor of the PIP joint. PI II moment arm was similar to ED II and slightly increases during PIP flexion. However, LU moment arm decreased on flexion of PIP. FDS

and FDP moment arms at MCP and PIP joints of all fingers (II, III, IV, V) followed a similar pattern and increased upon flexion of MCP and PIP joints. FDP moment arm at DIP joint upon flexion of DIP was slightly decreasing except for ring finger. Moment arms of ED III, IV and V at MCP, PIP and DIP joints, similar to ED II, were almost constant during MCP, PIP and DIP flexion. Similar to the index finger, intrinsic muscles of middle, ring and little fingers acted as a flexor of the MCP joint and as an extensor of the PIP joint (Figure 5).

Force evaluation

The FDS and FDP muscle-tendon forces of the index finger during pinch computed by the model were similar to forces obtained experimentally (Figure 6). The calculated FDP and FDS forces to applied fingertip force ratios were 2.5 and 2.3, respectively. These values were within the standard deviation of measured *in-vivo* forces; 2.2 ± 0.8 and 1.5 ± 1.0 for FDP and FDS reported by Kursu et al. (2005) for the slow rate loading condition.

Discussion

The main outcome of this study is the musculoskeletal model of the hand and wrist based on one coherent anatomical data set. The model yields similar

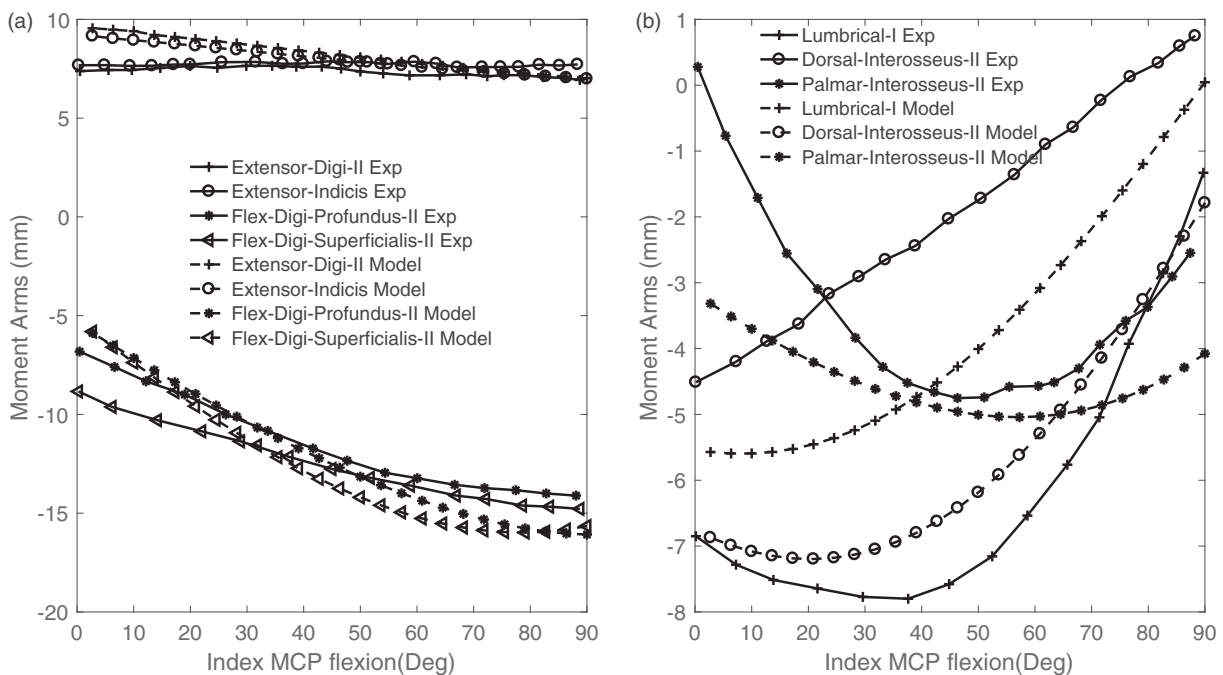


Figure 3. Comparison of model flexion–extension moment arms of MCP joint of the index finger during MCP movement (Model—dashed lines) with those experimentally measured (Exp—solid lines) (An et al. 1979). (a) extrinsic muscles; (b) intrinsic muscles.

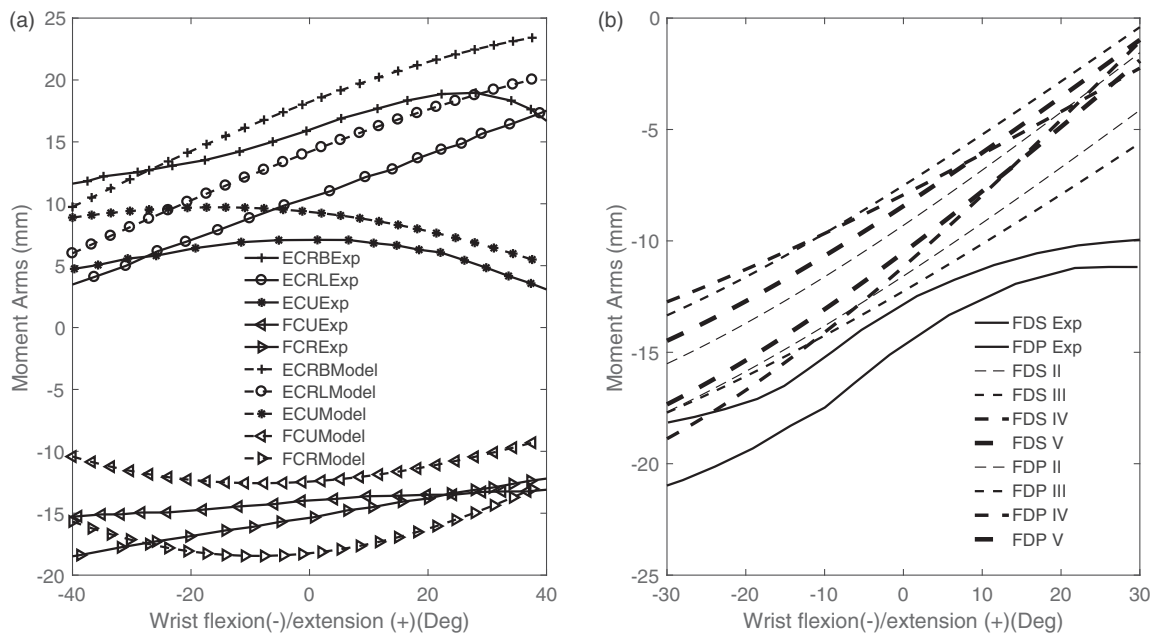


Figure 4. Model (dashed lines) and measured (Exp—solid lines) movement (Brand and Hollister 1999, Loren et al. 1996) moment arms at the flexion–extension axis of the wrist joint during flexion–extension wrist (see Table 1 for abbreviations of muscles).

patterns of calculated moment arms for muscles crossing index finger and wrist joint comparable to previously published moment arms (An et al. 1983) and muscle forces of FDP and FDS during a pinch task comparable to intra-operatively measured tendon forces, reported in literature (Kursa et al. 2005).

For the extrinsic muscles, the agreement between experimentally measured and computed moment arms was high. For the intrinsic muscles, the agreement was not as good. It should be noted that the presented experimental moment arms (Figure 3), as well as the quantitative comparison, were based on one representative cadaver, out of seven cadavers (An et al. 1983) since in that study only one cadaver moment arm acts as a function of joint angle were presented. The higher error for the intrinsic muscles can be explained by the differences in anthropometric data between cadavers (for instance middle phalanx length was 22.45 mm in the cadaver of our study and was 24.67 ± 1.37 mm in the cadavers measured by An et al. (1983)). In particular for the moment arm of the lumbrical this might explain why the computed moment arm of this muscle is not within inter-subject deviation (An et al. 1983) (Table 3). In a similar approach, Kocielek and Keir (2011) compared FDS and FDP moment arms using a different experimental protocol. They reported mean moment arms ranging between 11.9 and 12.7 mm, which were very close to the mean values in our study (Table 3). They showed that scaling can improve the model's outcome in term

of extrinsic muscle prediction, however, they did not study intrinsic muscles.

As expected from anatomical similarity of fingers, the moment arms of middle, ring and little finger followed a similar pattern as those of the index finger (Figure 5). In general, moment arms of muscles crossing little and ring finger had a lower magnitude than that of the index and middle finger.

For the flexion–extension axis of the wrist joint, moment arms were similar to previously reported wrist experimental data (Loren et al. 1996). However, poor correlations (FCU and FCR) and high deviation errors (ECRL and FDP at wrist) were observed (Table 2). This may be related to the high variability in experimental results (Loren et al. 1996). They only provided the upper and lower bands of moment arms, which varied substantially throughout the range of motion, indicating different patterns between cadavers. For instance, this difference ranged from around 3.4 to 0.7 mm for the FCU and 2.8 to 0.8 mm for the FCR. The poor correlation of the model's FCU and FCR moment arms with these measurements might therefore at least to some extent also be related to variability in experimental results.

It was shown in Figure 2 that extrinsic muscles can produce acceptable force in the finger and wrist range of motions. Considering the muscle force-length relationship and verified moment arms, these results implicitly indicate the capability of the muscles to produce reasonable active and passive joint moments within the range of movement.

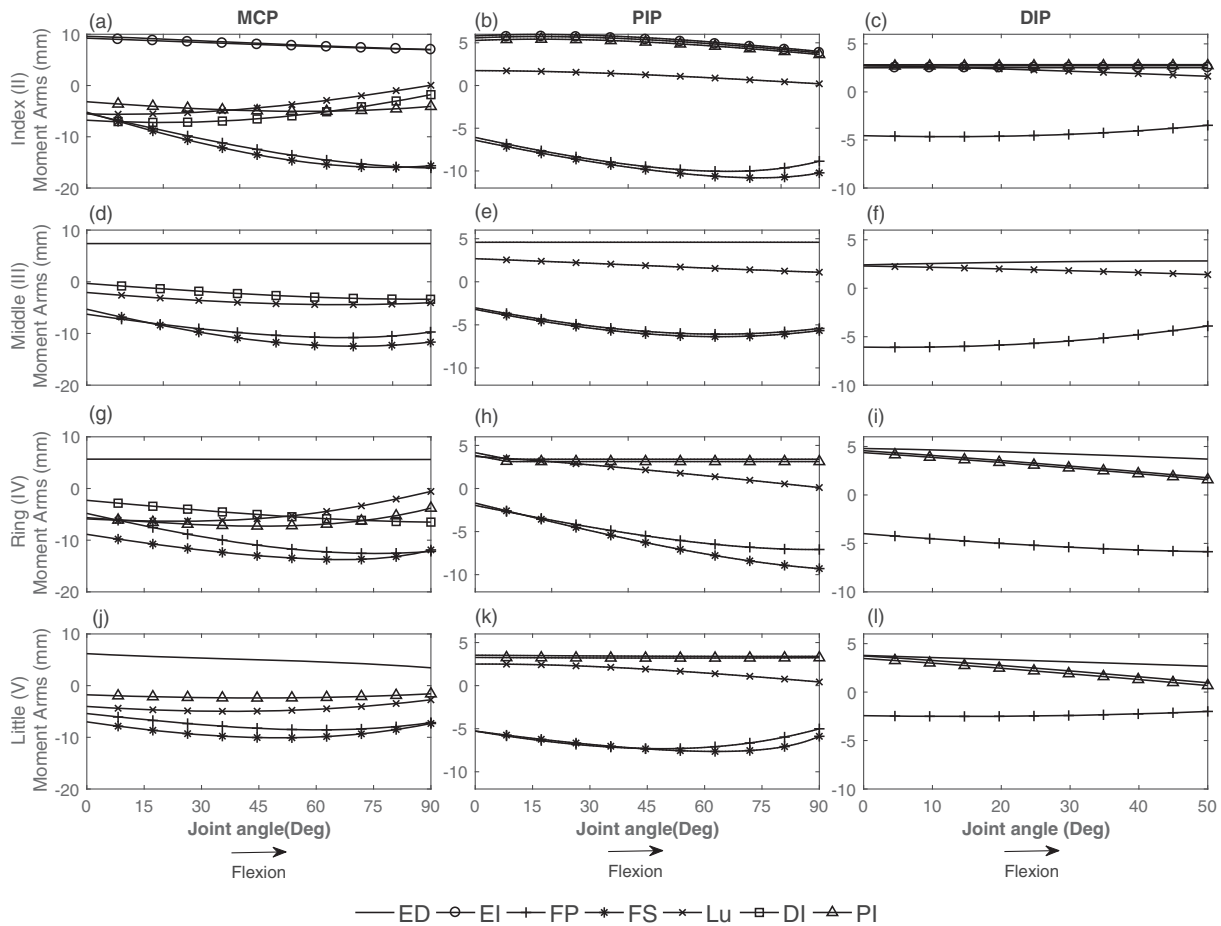


Figure 5. Moment arms of extrinsic and intrinsic muscles as a function of MCP (a, d, g, j), PIP (b, e, h, k) and DIP (c, f, i, l) joint angle.

Table 3. Muscle moment arms (mm) at MCP, PIP and DIP joints of the index finger computed by model and experimentally measured (mean \pm SD) (An et al. 1983).

	ED II	EI	FDS II	FDP II	LU I	DI I	PI II
MCP							
Experimental	8.6 ± 1.6	9.0 ± 1.3	-11.9 ± 0.7	-11.1 ± 1.1	-9.3 ± 2.1	-3.7 ± 1.4	-6.6 ± 2.1
Model	8.27	8.02	-12.6	-11.9	-3.5	-5.1	-5.3
PIP							
Experimental	2.8 ± 1.1	2.6 ± 1.1	-6.2 ± 1.0	-7.9 ± 1.1	1.8 ± 1.3	-	2.6 ± 0.8
Model	4.46	4.46	-9.37	-8.85	1.15	-	4.23
DIP							
Experimental	2.2 ± 0.4	1.9 ± 0.5	-	-4.1 ± 1.4	0.7 ± 0.6	-	1.6 ± 0.5
Model	2.83	2.83	-	-3.63	1.87	--	2.71

(-) Indicates flexion moment arms. Moment arms averaged over the range of imposed joint motions (See Table 1 for abbreviations of muscles). Moment arms reported by (An et al. 1983) (Table 3) were multiplied by 10, because we concluded that the values reported had to be in cm instead of mm.

The comparable discourses of computed and measured tendon forces during the pinch task provide further support to the validity of the developed model. Extrinsic flexor tendon forces computed during pinch were similar with *in vivo* recorded forces. In both cases, a comparable linear relationship between tendon and fingertip forces was found (Figure 6). Kursu et al. (2005) also reported *in-vivo* recorded force ratios of each subject. These ratios were similar for FDS and FDP for some subjects (ranging from

around 2 to 2.5), which compares closely to the similar force ratios of 2.5 and 2.3 for FDP and FDS computed by the presented model. Consistency of predicted and measured tendon forces is relevant to justify the extensor mechanism of the model. Intrinsic muscles contribute to the flexor moment at the MCP joint and act to balance the external moment at the PIP joint. All intrinsic muscles are active during pinch simulation, indicating that intrinsic muscles play a role in balancing the moments through the

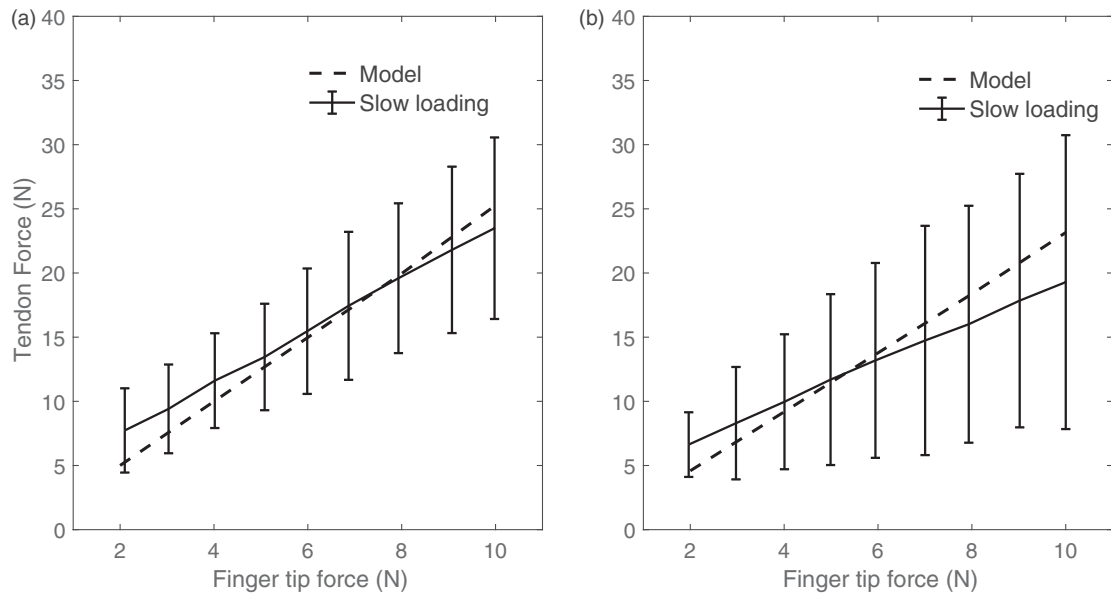


Figure 6. Comparison of FDP and FDS forces of model (dashed lines) and *in vivo* measurement (solid lines) (Kursa et al. 2005) during pinch by index finger.

extensor mechanism. There are other experimental studies measuring *in vivo* tendon force, such as Dennerlein et al. (1999). The applied fingertip force in their study, however, is slightly lower and has different pattern from Kursa et al. (2005), so it is not possible to compare measured *in-vivo* tendon force with predicted forces of our introduced model.

Our model is limited in some aspects. One single cadaver has the advantage of consistency but maybe limits the model in terms of its generalizability. Poor correlation of computed FCU and FCR moment arms with experimental ones and high errors for LU I might be due to errors in the measured attachment points of the data set (Mirakhorlo et al. 2016), inevitable simplification of the model in dividing muscles into straight line elements or lack of measured wrapping surface at the wrist. Simplification of wrist kinematics by ignoring the carpal bones may also play a role to the inaccuracies in the model's prediction of wrist moment arms. The wrist joint kinematics is complicated for modeling, not only due to the complex mechanical interaction of carpal bones but also due to cartilage layers and ligamentous structures (Fischli et al. 2009). The current model does not include the structures and therefore may impose inaccuracies to the computed moment arms. The limitation of the model to not accurately follow the complex structure of the extensor mechanism and consequently, the intrinsic muscles may also be partially responsible for the deviations between model and experimental moment arms of the index finger. More specifically, we did not include the lateral bands of the extensor

mechanism (Valero-Cuevas et al. 1998). The lateral bands connect the extensor digitorum to the extensor mechanism and were found to be pulled taut at particular finger joints angles (Li et al. 2001; Synek and Pahr 2016). In our model, the extensor digitorum was connected simply to the extensor mechanism at the distal part (Figure 1). Rotation of each individual finger joint affects the adjacent joint kinematics due to deformations in the joints pulleys which in turn, affect the reconstructed fingertip force from tendon forces (Dogadov et al. 2017). This simplification due to ignoring lateral bands has consequences for moment arm amplitude and also for force distribution and finger joint balances. This should be further elucidated in follow-up research. Furthermore, OpenSim only provides one type of cost function for optimization. In order to improve the model force predictions, other optimization approaches, such as new method introduced by (MacIntosh and Keir 2017) which account for co-contraction, may be used.

The current musculoskeletal model is one of the first-hand models that include the wrist and all the fingers and is based on a consistent anatomical data set. As the first step to evaluate the model, model performance was verified at the level of the computed moment arms of muscle crossing index and extrinsic flexors of the index finger during index pinch. Based on this verification, the model can, for example be used for investigating the wrist and finger interaction during static tasks. However, for other tasks such as unstable dynamic movements (Valero-Cuevas 2005), more specific validations will indeed be required.

The presented musculoskeletal model of hand and wrist can be a powerful tool to further improve our understanding of hand motor control. For example, the role of connections between tendons (Kilbreath and Gandevia 1994; Leijnse et al. 1997) or muscle bellies (Maas and Sandercock 2010) for controlling finger movements could be assessed. How such connections limit finger independence could be studied, however, this would require adding elements connecting tendons and/or muscle bellies. Furthermore, the model can provide more insight into hand–wrist mechanical interaction (as consequence of shared moment arms) and its effect on motor control of the fingers.

Disclosure statement

No potential conflict of interest was reported by the authors.

Funding

This research is funded by the European Commission through MOVE-AGE, an Erasmus Mundus Joint Doctorate program (2011-0015).

ORCID

H. E. J. Veeger  <http://orcid.org/0000-0003-0292-6520>

References

- Ackland DC, Lin YC, Pandy MG. 2012. Sensitivity of model predictions of muscle function to changes in moment arms and muscle-tendon properties: a Monte-Carlo analysis. *J Biomech.* 45:1463–1471.
- Allouch S, Boudaoud S, Younès R, Ben-Mansour K, Marin F. 2015. Proposition, identification, and experimental evaluation of an inverse dynamic neuromusculoskeletal model for the human finger. *Comput Biol Med.* 63:64–73.
- An KN, Chao EY, Cooney WP III, Linscheid RL. 1979. Normative model of human hand for biomechanical analysis. *J Biomech.* 12:775–788.
- An KN, Ueba Y, Chao E, Cooney W, Linscheid R. 1983. Tendon excursion and moment arm of index finger muscles. *J Biomech.* 16:419–425.
- Babikian S, Valero-Cuevas F, Kanso E. 2016. Slow movements of bio-inspired limbs. *J Nonlinear Sci.* 26:1293–1309.
- Bain G, Polites N, Higgs B, Heptinstall R, McGrath A. 2014. The functional range of motion of the finger joints. *IEEE Trans Biomed Eng.* 1753193414533754.
- Binder-Markey BI, Murray WM. 2017. Incorporating the length-dependent passive-force generating muscle properties of the extrinsic finger muscles into a wrist and finger biomechanical musculoskeletal model. *J Biomech.* 61:250–257.
- Brand PW, Hollister A. 1999. *Clinical mechanics of the hand* (Vol. 93). St. Louis: Mosby.
- Brook N, Mizrahi J, Shoham M, Dayan J. 1995. A biomechanical model of index finger dynamics. *Med Eng Phys.* 17:54–63.
- De Monsabert BG, Edwards D, Shah D, Kedgley A. 2018. Importance of consistent datasets in musculoskeletal modelling: a study of the hand and wrist. *Ann Biomed Eng.* 46:71–85.
- Delp SL, Anderson FC, Arnold AS, Loan P, Habib A, John CT, Guendelman E, Thelen DG. 2007. OpenSim: open-source software to create and analyze dynamic simulations of movement. *IEEE Trans Biomedical Eng.* 54:1940–1950.
- Dennerlein JT, Diao E, Mote C, Rempel DM. 1999. In vivo finger flexor tendon force while tapping on a keyswitch. *J Orthop Res.* 17:178–184.
- Dogadov A, Alamir M, Serviere C, Quaine F. 2017. The biomechanical model of the long finger extensor mechanism and its parametric identification. *J Biomech.* 58:232–236.
- Fischli S, Sellens R, Beek M, Pichora D. 2009. Simulation of extension, radial and ulnar deviation of the wrist with a rigid body spring model. *J Biomech.* 42:1363–1366.
- Garcia-Elias M, An K-N, Berglund L, Linscheid RL, Cooney WP, Chao EY. 1991. Extensor mechanism of the fingers. I. A quantitative geometric study. *J Hand Surg.* 16:1130–1136.
- Günal I, Köse N, Erdogan O, Göktürk E, Seber S. 1996. Normal range of motion of the joints of the upper extremity in male subjects, with special reference to side. *J Bone Joint Surg Am.* 78:1401–1404.
- Jacobson MD, Raab R, Fazeli BM, Abrams RA, Botte MJ, Lieber RL. 1992. Architectural design of the human intrinsic hand muscles. *J Hand Surg Am.* 17:804–809.
- Kilbreath S, Gandevia S. 1994. Limited independent flexion of the thumb and fingers in human subjects. *J Physiol.* 479:487–497.
- Kociolek AM, Keir PJ. 2011. Modelling tendon excursions and moment arms of the finger flexors: anatomic fidelity versus function. *J Biomech.* 44:1967–1973.
- Kursa K, Diao E, Lattanza L, Rempel D. 2005. In vivo forces generated by finger flexor muscles do not depend on the rate of fingertip loading during an isometric task. *J Biomech.* 38:2288–2293.
- Lee JH, Asakawa DS, Dennerlein JT, Jindrich DL. 2015. Finger muscle attachments for an OpenSim upper-extremity Model. *PLoS One.* 10:e0121712.
- Leijnse J, Walbeehm E, Sonneveld G, Hovius S, Kauer J. 1997. Connections between the tendons of the musculus flexor digitorum profundus involving the synovial sheaths in the carpal tunnel. *Cells Tissues Organs.* 160:112–122.
- Li Z-M, Zatsiorsky V, Latash M. 2001. The effect of finger extensor mechanism on the flexor force during isometric tasks. *J Biomech.* 34:1097–1102.
- Li Z-M. 2002. The influence of wrist position on individual finger forces during forceful grip. *J Hand Surg.* 27:886–896.

- Loren G, Shoemaker S, Burkholder T, Jacobson M, Friden J, Lieber R. 1996. Human wrist motors: biomechanical design and application to tendon transfers. *J Biomech.* 29:331–342.
- Maas H, Sandercock TG. 2010. Force transmission between synergistic skeletal muscles through connective tissue linkages. *BioMed Res Int.* 2010, 575672
- MacIntosh AR, Keir PJ. 2017. An open-source model and solution method to predict co-contraction in the finger. *Comput Methods Biomech Biomed Eng.* 20:1373–1381.
- Majors BJ, Wayne JS. 2011. Development and validation of a computational model for investigation of wrist biomechanics. *Ann Biomed Eng.* 39:2807.
- Mirakhorlo M, Visser JM, Goislard de Monsabert B, van der Helm F, Maas H, Veeger H. 2016. Anatomical parameters for musculoskeletal modeling of the hand and wrist. *Int Biomech.* 3:40–49.
- O'Brien TD, Reeves ND, Baltzopoulos V, Jones DA, Maganaris CN. 2010. In vivo measurements of muscle specific tension in adults and children. *Exp Physiology.* 95:202–210.
- O'Driscoll SW, Horii E, Ness R, Cahalan TD, Richards RR, An K-N. 1992. The relationship between wrist position, grasp size, and grip strength. *J Hand Surg.* 17:169–177.
- Park J, Han D-W, Shim JK. 2015. Effect of resistance training of the wrist joint muscles on multi-digit coordination. *Percept Motor Skills.* 120:816–840.
- Sancho-Bru JL, Mora MC, León BE, Pérez-González A, Iserte JL, Morales A. 2014. Grasp modelling with a biomechanical model of the hand. *Comput Methods Biomech Biomed Eng.* 17:297–310.
- Sancho-Bru, Perez-Gonzalez A, Vergara-Monedero M, Giurintano D. 2001. A 3-D dynamic model of human finger for studying free movements. *J Biomech.* 34:1491–1500.
- Synek A, Pahr D. 2016. The effect of the extensor mechanism on maximum isometric fingertip forces: a numerical study on the index finger. *J Biomech.* 49:3423–3429.
- Valero-Cuevas F, Johanson ME, Towles JD. 2003. Towards a realistic biomechanical model of the thumb: the choice of kinematic description may be more critical than the solution method or the variability/uncertainty of musculoskeletal parameters. *J Biomech.* 36:1019–1030.
- Valero-Cuevas FJ, Zajac FE, Burgar CG. 1998. Large index-fingertip forces are produced by subject-independent patterns of muscle excitation. *BioMed Mater Eng.* 31:693–703.
- Valero-Cuevas FJ. 2005. An integrative approach to the biomechanical function and neuromuscular control of the fingers. *J Biomech.* 38:673–684.
- Valero-Cuevas, Towles JD, Hentz VR. 2000. Quantification of fingertip force reduction in the forefinger following simulated paralysis of extensor and intrinsic muscles. *J Biomech.* 33:1601–1609.
- Vignais N, Marin F. 2014. Analysis of the musculoskeletal system of the hand and forearm during a cylinder grasping task. *Int J Ind Ergon.* 44:535–543.
- Vigouroux L, Domalain M, Berton E. 2009. Comparison of tendon tensions estimated from two biomechanical models of the thumb. *J Biomech.* 42:1772–1777.
- Wu J, An KN, Cutlip RG, Andrew ME, Dong RG. 2009. Modeling of the muscle/tendon excursions and moment arms in the thumb using the commercial software anybody. *J Biomech.* 42:383–388.
- Wu JZ, An KN, Cutlip RG, Dong RG. 2010. A practical biomechanical model of the index finger simulating the kinematics of the muscle/tendon excursions. *Bio-Med Mater Eng.* 20:89–97.